A subset of neurons controls the permeability of the peritrophic matrix and midgut structure in *Drosophila* adults

Hiroyuki Kenmoku[1], Hiroki Ishikawa[1, 2], Manabu Ote[1, 3], Takayuki Kuraishi[1, 4, 5, 6], and Shoichiro Kurata[1]

1. Department of Molecular Genetics, Graduate School of Pharmaceutical Sciences, Tohoku University, Sendai, Japan
2. Immune Signal Unit, Okinawa Institute of Science and Technology Graduate University, Japan
3. Division of Neurogenetics, Graduate School of Life Sciences, Tohoku University, Sendai, Japan
4. Department of Microbiology and Immunology, Keio University School of Medicine, Tokyo, Japan
5. Graduate School of Medical Sciences, Kanazawa University, Kanazawa, Ishikawa 920-1192, Japan
6. PRESTO, Japan Science and Technology Agency, Tokyo, Japan

Correspondence and requests for materials should be addressed to S.K.

Summary statement: Neuronal activity of a subset of neurons is required to maintain the organized proventricular structure and the physical barriers of the peritrophic matrix and epithelia in *Drosophila* gut.

Key words: Peritrophic matrix / *Drosophila* / enteric neurons

Abstract

The metazoan gut performs multiple physiologic functions, including digestion and absorption of nutrients, and also serves as a physical and chemical barrier against ingested pathogens and abrasive particles. Maintenance of these functions and structures is partly controlled by the nervous system, yet the precise roles and mechanisms of the neural control of gut integrity remain to be clarified in *Drosophila*. Here we screened for GAL4 enhancer-trap strains and labeled specific subsets of neurons. To inhibit their neuronal activity, we used Kir2.1. We identified an NP3253 line that is susceptible to oral infection by Gram-negative bacteria. The subset of neurons driven by the NP3253 line includes some of the enteric neurons innervating the anterior midgut, and these flies have a disorganized proventricular structure with high permeability of the peritrophic matrix and epithelial barrier. The findings of the present study indicate that neural control is crucial for maintaining the barrier function of the gut, and provide a route for genetic dissection of the complex brain-gut axis in the model organism *Drosophila* adults.

Journal of Experimental Biology • Advance article

Introduction

Maintaining the proper structure and function of the gastrointestinal tract is central to host homeostasis in metazoan animals. Aside from its main role in digestion and nutrient absorption, the gut must protect the animal from harmful substances and microorganisms, and thus acquires a strong immune system and develops physical/structural barriers against invaders (Sansonetti, 2004). The intestinal tract also appears to sense external cues, such as a nutrient availability, by the enteric endocrine or nervous system, and sends systemic signals though hormonal or neuronal means to change both metabolism and behavior (Furness and Costa, 1987). These functions of the intestinal tract are also consistent for most insects, including the model organism *Drosophila melanogaster* (Kuraishi et al., 2013; Lemaitre and Miguel-Aliaga, 2013).

Complex and highly organized tissue structures ensure the achievement of these important tasks of the gut. Compartmentalization, the sequential organization of regions that vary histologically and functionally, is an important feature of the intestinal tract (Karasov et al., 2011). In *Drosophila* adults, the gut is divided into three distinct domains based on the developmental origin: foregut, midgut, and hindgut. The midgut, the main region responsible for intestinal functions, comprises a single layer of epithelium, surrounded by visceral muscles, nerves, and tracheae, and is subdivided into six major anatomic regions with distinct functions (Buchon et al., 2013b).

The peritrophic matrix and septate junctions between epithelial cells have a central role as a physical barrier against external invaders (Hegedus et al., 2009; Tepass et al., 2001). The peritrophic matrix is an acellular structure that forms a layer of chitin polymers and glycoproteins, such as peritrophins, lining the insect midgut lumen (Lehane, 1997). The peritrophic matrix seems to be formed by either the midgut epithelium (Type I) or the proventriculus (Type II), a specialized structure located at the foregut/midgut junction that regulates food passage to the midgut. In type I peritrophic matrix, delamination of successive concentric lamellae occurs along the length of the midgut. Diptera such as *Drosophila* have a type II peritrophic matrix that is continuously produced by specific cells of the proventriculus (King, 1988). The protective role of the peritrophic matrix against abrasive food particles and pathogens as well as in sequestering ingested toxins has been studied in many insects (Edwards and Jacobs-Lorena, 2000; Wang and Granados, 2000). In *Drosophila* adults,

mutation in the *drosocrystallin* (*dcy*) gene, which codes for a structural component of the peritrophic matrix, results in reduced thickness and higher permeability of the peritrophic matrix (Kuraishi et al., 2011). The *dcy* mutant flies show greater susceptibility to ingested entomopathogenic bacteria or pore-forming toxins. The septate junctions are functionally related to mammalian tight junctions and participate in epithelial barrier function, i.e., protecting the fly from oral infection by pathogenic bacteria. Bonnay et al. demonstrated that the *big bang gene* (*bbg*) encodes a PDZ domain-containing protein that presents at the level of the septate junctions (Bonnay et al., 2013). A mutation in *bbg* results in the loosening of septate junctions, and is associated with acute susceptibility to invasive enteric pathogens such as *Pseudomonas aeruginosa* and *Serratia marcescens*. The compartmentalization, peritrophic matrix, and septate junctions of the gut are maintained throughout adult life by rapid turnover of the epithelium in 1 to 2 weeks under steady-state conditions (Buchon et al., 2013a; Buchon et al., 2013b). The cellular and molecular processes required to maintain these cellular and acellular structures of the intestinal tract, however, are poorly understood.

A major function of the stomatogastric nervous system is to control peristalsis of the muscles surrounding the intestinal tract (Huizinga and Lammers, 2009), and to sense external conditions to regulate metabolism. A recent study in *Drosophila* adults revealed that enteric neurons also govern fluid homeostasis and sex peptide-induced changes in intestinal physiology, pointing to an indispensable role for the brain-gut axis in maintaining host homeostasis (Cognigni et al., 2011; Talsma et al., 2012). We hypothesized that the enteric nervous system also has a role in maintaining the structural integrity of the gut, which is important for its barrier function.

In this study, we identified a subset of neurons required for maintaining gut impermeability against enteric pathogens, providing evidence for the neural control of gut integrity in *Drosophila* adults.

Materials and Methods

Fly stocks

Oregon R flies were used as wild-type flies. The GAL4 lines screened in this study were obtained from the Bloomington Stock Center (Indiana University, Bloomington, IN, USA) and, Drosophila Genetic Resource Center (Kyoto Institute of Technology, Japan) and *384-GAL4, Bx-GAL4, elav-GAL4, tubP-GAL80^{ts}, L^{1}/CyO ; UAS-DenMark, syt.eGFP* and *UAS-mCD8::GFP/CyO* were from Bloomington Stock Center. *UAS-dTrpA1* was a gift from P. Garrity (Hamada et al., 2008). *elav-GAL80* was a gift from Y. Jan (Yang et al., 2009). *UAS-lacZ* (Bloomington Drosophila Stock Center) or *w^{1118}* was used as a control. *Drosophila* stocks and crosses were maintained at 18°C or 25°C in tubes containing standard cornmeal-agar medium. To inhibit or activate neural activity, 5 to 9-day-old flies of *NP3253-GAL4/tubP-GAL80^{ts}; UAS-Kir2.1-EGFP* (Baines et al., 2001)*/+* (*NP3253>Kir2.1* flies), or *NP3253-GAL4/UAS-dTrpA1* were maintained at 30°C for 2 days prior to use in all experiments. The NP3253 line was subjected to standard mitotic recombination over *y w* chromosomes to eliminate possible second-site mutations.

Microbial infection

The *Ecc15-GFP* strain was described previously (Basset et al., 2000) and was grown in Luria Bertani broth for all experiments. Flies were grown at 29-30°C and allowed to reach the stationary phase. Cells were then concentrated at OD_{600}= 200 with 2.5% sucrose solution. For oral infection, flies were starved for 2 h at 30°C and then placed in a fly vial with food solution. The food solution was made by mixing a pellet of bacteria, added to a filter disk that completely covered the surface of standard fly medium. Flies were maintained at 30°C and survival was monitored at different time points.

Immunohistochemistry

Drosophila adults were dissected into cold phosphate-buffered saline (PBS), and the guts or brains were immediately fixed with 4% paraformaldehyde in PBS for 30 min at room temperature. The samples were rinsed in 0.5% TritonX-100 in PBS, and then incubated with primary antibodies (dilution 1:500 rabbit anti-GFP (Invitrogen, Carlsbad, CA, USA), 1:500 mouse anti-GFP (Invitrogen), 1:500 rabbit anti-RFP (Invitrogen), 1:500 rabbit anti-PH3 9701 (Cell Signaling, Danvers, MA), 1:100 mouse anti-Discs-large 4F3 (Developmental Studies Hybridoma Bank), 1:500 Alexa647-conjugated goat anti-HRP antibody (Jackson ImmunoResearch, West Grove, PA, USA) in 0.5% TritonX-100 in PBS at 4°C overnight. The samples were then washed twice with 0.2% TritonX-100 in PBS, and primary antibodies were labeled with Alexa488-, Alexa 546- or Alexa647-coupled secondary antibodies (Invitrogen). Actin filaments were stained with Rhodamine-Phalloidin (dilution 1:100 [Sigma-Aldrich, St. Louis, MO, USA]) and nuclei were stained with DAPI (3 μg/mL, DOJINDO, Japan). The samples were then washed with 0.2% TritonX-100 in PBS, incubated with 50% glycerol (Wako, Japan) in PBS, and mounted in 80% glycerol in PBS or in VECTASHELD. For anti-PH3 antibody staining, the samples were fixed with 3.7% formaldehyde in PBS, permeabilized with 99.5% pre-chilled EtOH at -30℃ for 5 min. The samples were visualized with a Leica TCS-SPE confocal microscope, and images were reconstructed using Photoshop (Adobe) and ImageJ.

For quantification of PH3-positive cells, PH3-positive cells in whole midgut of 10 to 12 female flies were counted under a confocal microscope. For quantification of the proventriculus or midgut areas in Figure 4, confocal images that showed the maximum measured area were obtained, and the areas were calculated by Image J in the area of luminal region of proventriculus, or the area of the anterior midgut (from the top of the proventriculus to the 200-μm point).

Feeding assay with FITC-labeled beads

Flies were starved for 2 h at 30℃, fed with FITC-labeled beads (50 nm diameter, Polysciences, Inc., Warrington, PA, USA) to monitor the permeability of the peritrophic matrix, as described previously (Kuraishi et al., 2011). Images were captured with a Zeiss

conventional fluorescence microscope or a Leica confocal microscope with a 1.5 AU pinhole. For quantification, the guts were dissected out 10 min after feeding and observed under a conventional fluorescence microscope using 20 to 30 female flies.

β-glo assay

Five pairs of the salivary glands were dissected out from adult flies in 50 µL of PBS, homogenized with pestle, added 350 µL of PBS and 50 µL of PBS containing 5% of Triton X-100, incubated for 10 min at room temperature, and diluted 100 times with PBS. Fifty microliters of diluted samples was mixed with 10 times-diluted β-glo reagent (Promega), incubated for 30 min, and emission at 570 nm was measured by a luminometer. Assays were performed on triplicate samples.

BPB feeding assay

Assays were performed largely based on the published method (Cognigni et al Cell Metab., 2011). For quantification of the feeding amount, three female flies were starved for 3 h at 30℃, fed with 0.5% BPB sodium salt/cornmeal-agar for 1 or 2 h, and then each fly was placed into 50 µL of MilliQ water, homogenized with pestle, and centrifuged twice to remove debris. Absorption at 594 nm was measured using a NANODROP2000 (Thermo Scientific, Waltham, MA). For quantification of the excretion rate, five female flies were starved for 3 h at 30℃, fed with 0.5% BPB sodium salt/cornmeal-agar for 1 h at 30℃, moved to a new vial containing normal food and maintained there for several hours. Each fly was placed into 80 µL of MilliQ, homogenized with pestle, and centrifuged twice to remove debris. Absorption at 594 nm was measured using the NANODROP2000.

Lifespan analysis

All flies were raised at 18℃ for 5 to 6 days after eclosion. Three vials (each containing 30 flies) were moved to 30℃. After 2 days, lifespan analysis was started (set this day to day 0) at 30℃. Live flies were counted every day and transferred to new vials every 2 days.

Statistical analysis

Statistical analyses were performed using Student's t test or the log–rank test, and *P* values less than 0.05 were considered significant.

Results

NP3253-positive cells are required for defense against bacterial oral infection

To identify neurons important for gut integrity, we screened GAL4 enhancer trap lines with Kir2.1, a mammalian inwardly rectifying K^+ channel, to block neural activity (Baines et al., 2001), and examined their susceptibility to oral bacterial challenge as a measure of gut integrity. Sensitivity to bacterial infection is a complex phenomenon (Ayres and Schneider, 2012; Lemaitre and Hoffmann, 2007), as not only resistance mechanisms, such as the expression of antimicrobial peptides, but also tolerance mechanisms, such as permeability of the epithelial barrier, feeding behavior, excretion of ingested materials, and damage repair after infection, are required for normal survival upon infection (Buchon et al., 2013a; Kuraishi et al., 2013). Therefore, if some lines are susceptible to oral infection, the underlying mutations are expected to be involved in some aspect of gut function, including structural integrity.

We selected 350 GAL4 enhancer trap lines **(Table 1)** known to induce expression in neurons based on the FLYBRAIN and Flytrap databases (Kelso et al., 2004; Shinomiya et al., 2011). Kir2.1 expression was repressed by a temperature-sensitive GAL80 ($GAL80^{ts}$) until adulthood and then induced by shifting the flies to a restrictive temperature for 2 days **(Fig. 1A)**. Several enhancer trap lines that expressed Kir2.1 were susceptible to *Ecc15* oral infection **(Fig. 1B)**. Of those, a fly line expressing Kir2.1 by NP3253-GAL4, designated *NP3253>Kir2.1* flies, exhibited strong susceptibility to *Ecc15* oral infection, but not to normal fly foods **(Fig. 1C, D)**. In contrast, flies with hyperactive NP3253-positive cells by the expression of dTrpA1 (Rosenzweig et al., 2005) were not sensitive to *Ecc15* oral infection **(Fig. 1E)**. To exclude the possibility that these phenotypes resulted from the genetic background, the NP3253 line was backcrossed with the *y w* strain, and the Kir2.1-induced susceptibility was tested upon oral infection with *Ecc15*. The findings demonstrated that

these flies were also susceptible to infection **(Fig. 1C, D)**, indicating that the activity of NP3253-positive cells is specifically required for gut defense upon bacterial infection.

NP3253-positive neurons are responsible for the survival phenotype

We next examined the expression pattern in the tissues of adult flies to evaluate whether NP3253-GAL4 could induce expression in enteric neurons. Many green fluorescent protein (GFP)-positive cells driven by NP3253-GAL4 were detected in the brain, proventriculus, and anterior midgut, as well as in the posterior midgut **(Fig. 2A and B)**, salivary glands, trachea, and reproductive organs (data not shown). A previous study (Tanaka et al., 2008) reported that NP3253 labels neurons in the mushroom body. To analyze whether the NP3253-positive cells in the gut are neurons, they were stained with horseradish peroxidase (HRP), a neural marker protein, together with anti-GFP. The GFP-positive cells driven by NP3253-GAL4 in the proventriculus and anterior midgut were HRP-positive, whereas those in posterior midgut were not **(Fig. 2C)**. NP3253-positive cells in the proventriculus and anterior midgut were positive for the synaptic vesicle marker Syt.eGFP and the dendrite marker DenMark **(Fig. 2D and E)**. These findings suggest that NP3253-positive cells in the proventriculus and anterior midgut are neurons, and indicate that not all NP3253-positive cells are neurons. This led us to examine whether NP3253-positive neurons are responsible for the survival phenotype upon *Ecc15* oral infection. We analyzed *NP3253>Kir2.1* flies in combination with *elav-GAL80* to inhibit GAL4 activity in all neurons (Rideout et al., 2010). Survival analysis revealed that susceptibility to *Ecc15* oral infection was partially rescued by co-expression with *elav-GAL80* **(Fig. 2F)**. Both *NP3253-GAL4* and *elav-GAL80* drive gene expression in the salivary gland **(Fig. 2G)**; therefore, to rule out the possibility that the salivary gland is responsible for the survival phenotype, we used Bx-GAL4 and 384-GAL4 to drive Kir2.1. Both drivers induced reporter expression in the salivary gland as strong as NP3253-GAL4 **(Fig. 2G and H)**, but *Bx>Kir2.1* flies nor *384>Kir2.1* flies were not susceptible to oral infection with *Ecc15* **(Fig. 2I and J)**. Together these results suggest that a subset of neurons driven by NP3253-GAL4 is partly involved in the survival phenotype.

The gut barriers of NP3253>Kir2.1 flies are highly permeable

Next, we examined why the *NP3253>Kir2.1* flies exhibit sensitivity to bacterial oral infection. After feeding the flies GFP-labeled *Ecc15* (*Ecc15-GFP*), GFP signals were observed in the whole body of *NP3253>Kir2.1* flies, in contrast to wild-type flies, which expressed the GFP signal only in the abdomen **(Fig. 3A)**. GFP signals were observed throughout the whole body in ~10% of the *NP3253>Kir2.1* flies at 6 h after *Ecc15-GFP* feeding and in up to 20% at 24 h after *Ecc15-GFP* feeding **(Fig. 3B)**. This observation indicated that the bacteria intruded into the hemolymph of *NP3253>Kir2.1* flies, suggesting that gut barrier function was compromised in these flies. The peritrophic matrix is an acellular layer that protects the gut epithelium, and its permeability can be assessed by feeding adults fluorescein isothiocyanate (FITC)-labeled beads (Kuraishi et al., 2011). Conventional fluorescence microscopy revealed that the 50-nm FITC-labeled beads remained in the lumen of wild-type flies after feeding **(Fig. 3C and D)**. In contrast, FITC signals were diffuse in the gut of *NP3253>Kir2.1* flies **(Fig. 3C and D)**. Close examination using a confocal microscope with the focal plane on the epithelial cells **(Fig. 3E)** revealed FITC signals outside the peritrophic matrix in the *NP3253>Kir2.1* flies **(Fig. 3F)**. Consistent with these observations, staining with the mitotic marker PH3 revealed that upd3-dependent stem cell proliferation, an indicator of gut damage, was increased in the midgut of *NP3253>Kir2.1* flies **(Fig 3G and H)**. Furthermore, *NP3253>Kir2.1 flies* had a shorter lifespan, and began to die 1 to 2 weeks after emergence **(Fig. 3I)**. Indeed, Rera et al. reported that increased gut permeability is a cause and predictor of imminent death (Rera et al., 2012). These findings indicate that the peritrophic matrix of *NP3253>Kir2.1* flies is more permeable or broken, providing an explanation for the susceptibility of *NP3253>Kir2.1* flies to oral infection.

Gut structure and function of NP3253>Kir2.1 flies

We then performed histologic analysis of the gut of *NP3253>Kir2.1* flies. The proventriculus, the organ responsible for secretion of the peritrophic matrix in *Drosophila* adults, was stained with phalloidin and 4',6-diamidino-2-phenylindole (DAPI) to visualize the actin filaments and nuclei, respectively. As shown in **Figure 4A and B,** the proventriculus morphology in *NP3253>Kir2.1* flies differed from that in wild-type flies: the bulge formed

by the inner cells (indicated by arrowheads) was lost in *NP3253>Kir2.1* flies, whereas the top of the inner part of the proventriculus was expanded (indicated by the arrows). This observation was supported by visualizing the tissue structure following staining with the marker for cell junctions, discs-large **(Fig. 4C)**. These findings indicated that a part of the proventriculus of *NP3253>Kir2.1* flies was flattened **(Fig. 4D).** We also observed a morphologic abnormality of the midgut of *NP3253>Kir2.1* flies. The diameter of the anterior part of the midgut, especially the R1 region of the midgut (Buchon et al., 2013b), was increased without a significant change in the number and shape of epithelial cells **(Fig. 4E and F)**. This phenotype was also observed in starved *NP3253>Kir2.1* flies. Notably, the increased diameter of the anterior midgut was also observed in the upd3 mutant background **(Fig. 4G)**, suggesting that the increased diameter is not due to damage-induced stem cell proliferation. We further examined the feeding and excretion of the *NP3253>Kir2.1* flies. As shown in Figure 5, neither the feeding nor the excretion rate of *NP3253>Kir2.1* flies, quantified by the amount of BPB food dye that flies ate, was compromised. These results suggest that the increased diameter was not due to defective excretion of the foods they had eaten, but rather to the homeostatic dysfunction of the *NP3253>Kir2.1* flies to maintain normal gut morphology.

Discussion

The stomatogastric nervous system controls peristalsis, fluid homeostasis, and sex peptide-induced changes in intestinal physiology in adult *Drosophila*. Here we describe a role of the nervous system in maintaining the impermeable gut physical barrier and organized epithelial structure of the anterior midgut. Several questions remain, however, as discussed below.

The type of defect of the peritrophic matrix and epithelial barrier

We demonstrated that the peritrophic matrix of *NP3253>Kir2.1* flies is more permeable than that of wild-type flies. This phenotype is much stronger than that of dcy^1 mutant flies. The peritrophic matrix of dcy^1 mutant flies is not permeable to FITC-labeled beads with a size >70 kDa (Kuraishi et al., 2011). The peritrophic matrix of the *NP3253>Kir2.1* flies, however, was permeable not only to latex beads, but also to bacteria, implying that the nature of the peritrophic matrix defects of *NP3253>Kir2.1* flies differs from that of the dcy^1 mutant.

What is the defect that occurs in the epithelial barrier? We observed that the epithelial structure of the proventriculus and anterior midgut was disorganized and expanded in *NP3253>Kir2.1* flies. We speculate that ingested bacteria augment the epithelial expansion and might affect the septate junctions between epithelial cells, resulting in a leaky epithelial barrier in the flies. This possibility should be examined in future studies.

The nature of NP3253-positive neurons and mechanisms of control of` structural integrity

NP3253-GAL4 drives expression in neuronal subsets in the brain and the anterior midgut in *Drosophila* adults. It is unclear which NP3253-positive neurons are involved in the observed phenotype and whether efferent or sensory neurons are responsible. We cannot rule out the possibility that NP3253-positive neurons only in the brain, and not enteric neurons, are responsible for the observed phenotype. Further screening of enhancer trap lines is needed to identify drivers that have a similar phenotype as NP3253-GAL4.

Our study does not address the mechanisms of the NP3253-positive neurons that maintain the impermeability of the epithelial barrier and morphology. A possible mechanism

by which NP3253-positive neurons control gut integrity is endocrine/paracrine regulation. Gut patterning is primarily achieved through interactions between the pan-midgut and region-specific transcription factors, together with spatial activities of morphogens (Buchon et al., 2013b). It is thus possible that secreted factors from NP3253-positive neurons affect morphogen expression or the activities of transcriptional factors in the anterior midgut. Although we showed that peristalsis is not severely compromised in the *NP3253>Kir2.1* flies, another possibility is that NP3253-positive neurons control the pumping action of the proventriculus. The secreted components of the peritrophic matrix from the cells of the proventriculus are squeezed to form the peritrophic matrix sleeve and conveyed throughout the midgut by pumping of the proventriculus (Lehane, 1997). Therefore, if the activity of NP3253-positive neurons is inhibited, the peritrophic matrix does not form correctly or smoothly, and thus may accumulate around the anterior midgut, leading to an enlarged and abnormal structure with compromised permeability of the gut barriers. Because constitutive activation of NP3253-positive cells does not induce susceptibility to *Ecc15* oral infection **(Fig. 1D)**, the latter explanation is more plausible.

Acknowledgements

We are grateful to Dr. B. Lemaitre for *Ecc15-GFP*. We thank Drs. P. Garrity and Y. Jan at the Bloomington Stock Center (NIH P40OD018537), the Drosophila Genomics Resource Center at Indiana University, the Drosophila Genetic Resource Center at the Kyoto Institute of Technology, the Drosophila RNAi Screening Center, the Genetic Strain Research Center of National Institute of Genetics, and the Vienna Drosophila RNAi Center for fly stocks. We also thank the Developmental Studies Hybridoma Bank for antibodies; and FlyBase, FLYBRAIN, Flytrap, and FlyAtlas for use of the databases.

Author contributions

H. K. performed many of the experiments in this study with input from M. O., T. K., and S. K. H. I. performed screening for enhancer trap lines. M.O. took the picture of the brain-gut neurons. All authors analyzed the data. H. K. and T. K. wrote the draft, and all authors finalized the manuscript.

The authors declare no conflict of interest.

Funding

This work was supported by grants from the Japan Science and Technology Agency (JST); the Ministry of Education, Culture, Sports, Science, and Technology of Japan (MEXT); the Kao Foundation for Arts and Sciences; the Uehara Memorial Foundation; and the Futaba Electronics Memorial Foundation.

References

Ayres, J. S. and Schneider, D. S. (2012). Tolerance of infections. *Annu. Rev. Immunol.* **30**, 271-94.

Baines, R. A., Uhler, J. P., Thompson, A., Sweeney, S. T. and Bate, M. (2001). Altered electrical properties in Drosophila neurons developing without synaptic transmission. *J. Neurosci.* **21**, 1523-31.

Basset, A., Khush, R. S., Braun, A., Gardan, L., Boccard, F., Hoffmann, J. A. and Lemaitre, B. (2000). The phytopathogenic bacteria Erwinia carotovora infects Drosophila and activates an immune response. *Proc. Natl. Acad. Sci. U. S. A.* **97**, 3376-81.

Bonnay, F., Cohen-Berros, E., Hoffmann, M., Kim, S. Y., Boulianne, G. L., Hoffmann, J. A., Matt, N. and Reichhart, J. M. (2013). big bang gene modulates gut immune tolerance in Drosophila. *Proc. Natl. Acad. Sci. U. S. A.* **110**, 2957-62.

Buchon, N., Broderick, N. A. and Lemaitre, B. (2013a). Gut homeostasis in a microbial world: insights from Drosophila melanogaster. *Nat. Rev. Microbiol.* **11**, 615-26.

Buchon, N., Osman, D., David, F. P., Fang, H. Y., Boquete, J. P., Deplancke, B. and Lemaitre, B. (2013b). Morphological and molecular characterization of adult midgut compartmentalization in Drosophila. *Cell Rep.* **3**, 1725-38.

Cognigni, P., Bailey, A. P. and Miguel-Aliaga, I. (2011). Enteric neurons and systemic signals couple nutritional and reproductive status with intestinal homeostasis. *Cell Metab.* **13**, 92-104.

Edwards, M. J. and Jacobs-Lorena, M. (2000). Permeability and disruption of the peritrophic matrix and caecal membrane from Aedes aegypti and Anopheles gambiae mosquito larvae. *J. Insect Physiol.* **46**, 1313-1320.

Furness, J. B. and Costa, M. (1987). The enteric nervous system. London: Churchhill-Livingstone.

Hamada, F. N., Rosenzweig, M., Kang, K., Pulver, S. R., Ghezzi, A., Jegla, T. J. and Garrity, P. A. (2008). An internal thermal sensor controlling temperature preference in Drosophila. *Nature* **454**, 217-20.

Hegedus, D., Erlandson, M., Gillott, C. and Toprak, U. (2009). New insights into peritrophic matrix synthesis, architecture, and function. *Annu. Rev. Entomol.* **54**, 285-302.

Huizinga, J. D. and Lammers, W. J. (2009). Gut peristalsis is governed by a multitude of cooperating mechanisms. *Am. J. Physiol. Gastrointest. Liver Physiol.* **296**, G1-8.

Karasov, W. H., Martinez del Rio, C. and Caviedes-Vidal, E. (2011). Ecological physiology of diet and digestive systems. *Annu. Rev. Physiol.* **73**, 69-93.

Kelso, R. J., Buszczak, M., Quinones, A. T., Castiblanco, C., Mazzalupo, S. and Cooley, L. (2004). Flytrap, a database documenting a GFP protein-trap insertion screen in Drosophila melanogaster. *Nucleic Acids Res.* **32**, D418-20.

King, D. G. (1988). Cellular organization and peritrophic membrane formation in the cardia (proventriculus) of Drosophila melanogaster. *J. Morphol.* **196**, 253-82.

Kuraishi, T., Binggeli, O., Opota, O., Buchon, N. and Lemaitre, B. (2011). Genetic evidence for a protective role of the peritrophic matrix against intestinal bacterial infection in Drosophila melanogaster. *Proc. Natl. Acad. Sci. U. S. A.* **108**, 15966-71.

Kuraishi, T., Hori, A. and Kurata, S. (2013). Host-microbe interactions in the gut of Drosophila melanogaster. *Front. Physiol.* **4**, 375.

Lehane, M. J. (1997). Peritrophic matrix structure and function. *Annu. Rev. Entomol.* **42**, 525-50.

Lemaitre, B. and Hoffmann, J. (2007). The host defense of Drosophila melanogaster. *Annu. Rev. Immunol.* **25**, 697-743.

Lemaitre, B. and Miguel-Aliaga, I. (2013). The digestive tract of Drosophila melanogaster. *Annu. Rev. Genet.* **47**, 377-404.

Rera, M., Clark, R. I., and Walker, D. W. (2012). Intestinal barrier dysfunction links metabolic and inflammatory markers of aging to death in Drosophila. *Proc. Natl. Acad. Sci. U S A.* **109**, 21528-33.

Rideout, E. J., Dornan, A. J., Neville, M. C., Eadie, S. and Goodwin, S. F. (2010). Control of sexual differentiation and behavior by the doublesex gene in Drosophila melanogaster. *Nat. Neurosci.* **13**, 458-66.

Rosenzweig, M., Brennan, K. M., Tayler, T. D., Phelps, P. O., Patapoutian, A. and Garrity, P. A. (2005). The Drosophila ortholog of vertebrate TRPA1 regulates thermotaxis. *Genes Dev.* **19**, 419-24.

Sansonetti, P. J. (2004). War and peace at mucosal surfaces. *Nat. Rev. Immunol.* **4**, 953-64.

Shinomiya, K., Matsuda, K., Oishi, T., Otsuna, H. and Ito, K. (2011). Flybrain neuron database: a comprehensive database system of the Drosophila brain neurons. *J. Comp. Neurol.* **519**, 807-33.

Talsma, A. D., Christov, C. P., Terriente-Felix, A., Linneweber, G., Perea, D., Wayland, M., Shafer, O. and Miguel-Aliaga, I. (2012). Remote control of renal physiology by the intestinal neuropeptide pigment-dispersing factor in Drosophila. *Proc. Natl. Acad. Sci. U. S. A.* **109**, 12177-12182.

Tanaka, N. K., Tanimoto, H. and Ito, K. (2008). Neuronal assemblies of the Drosophila mushroom body. *J. Comp. Neurol.* **508**, 711-55.

Tepass, U., Tanentzapf, G., Ward, R. and Fehon, R. (2001). Epithelial cell polarity and cell junctions in Drosophila. *Annu. Rev. Genet.* **35**, 747-84.

Wang, P. and Granados, R. R. (2000). Calcofluor disrupts the midgut defense system in insects. *Insect Biochem. Mol. Biol.* **30**, 135-43.

Yang, C. H., Rumpf, S., Xiang, Y., Gordon, M. D., Song, W., Jan, L. Y. and Jan, Y. N. (2009). Control of the postmating behavioral switch in Drosophila females by internal sensory neurons. *Neuron* **61**, 519-26.

Figures

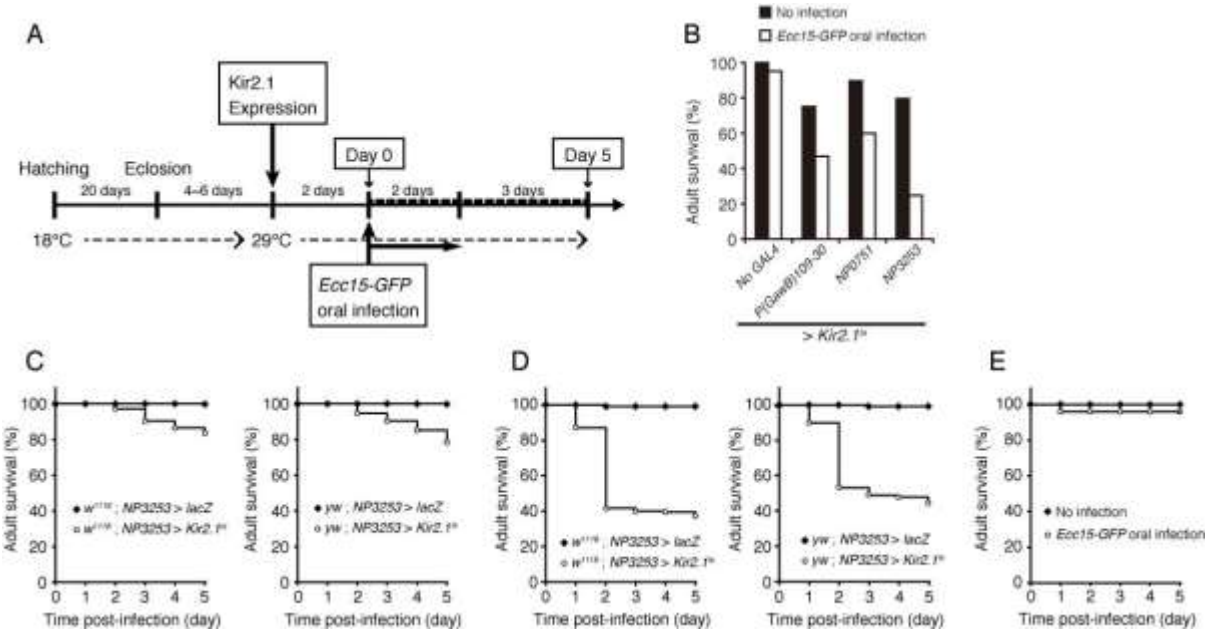

Figure 1.

NP3253>Kir2.1 flies are susceptible to oral infection with *Ecc15-GFP*. **(A)** Time table for neuronal inhibition by Kir2.1. Kir2.1 was expressed with temperature-sensitive GAL80, and the expressed flies were raised at 18°C until adulthood. They were moved at 29°C and kept for 2 days before oral infection with *Ecc15-GFP*. The flies were maintained in vials with *Ecc15-GFP* for 2 days, and then moved to standard medium. **(B)** Survival analysis of Kir2.1-expressing flies by several GAL4 driver lines upon oral infection with *Ecc15-GFP*. Graph shows the survival rate of ~30 flies 3 days after infection. **(C)** Survival analysis of *NP3253>lacZ* or *NP3253>Kir2.1* flies upon sucrose feeding. NP3253 is w^{1118} background (Left) or *y w* background (Right). **(D)** Survival analysis of *NP3253>lacZ* or *NP3253>Kir2.1* flies orally infected with *Ecc15-GFP*. *NP3253* is w^{1118} background (Left) or *y w* background (Right) $P<0.0001$ (left and right, comparing *NP3253>lacZ* with *NP3253>Kir2.1*). **(E)** Survival analysis of *NP3253>dTrpA1* flies orally infected with *Ecc15-GFP*. No infection indicates sucrose feeding after starvation. Each survival curve corresponds to at least 2 independent experiments of 3 tubes of 30 flies each. *P* values were calculated with the log-rank test.

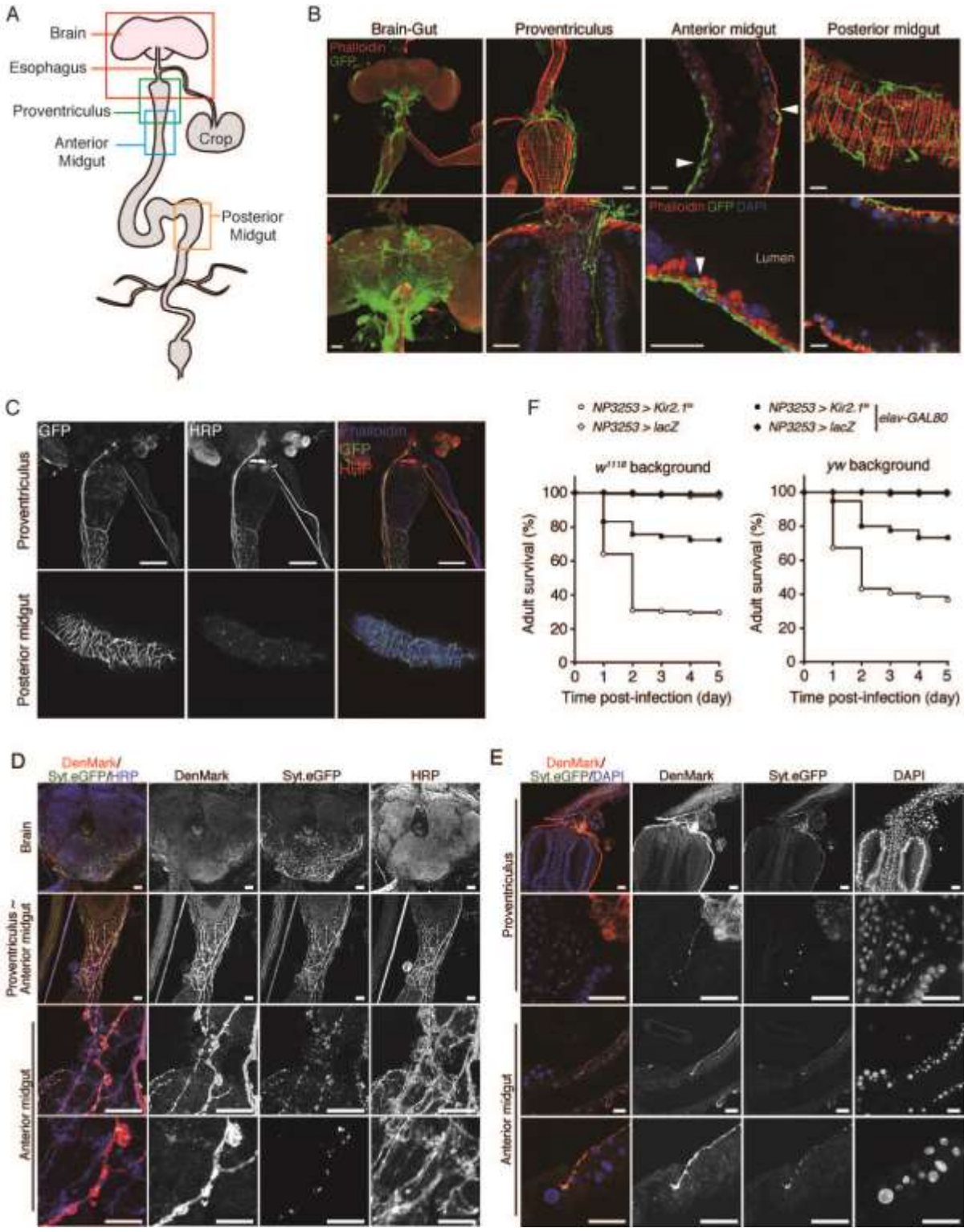

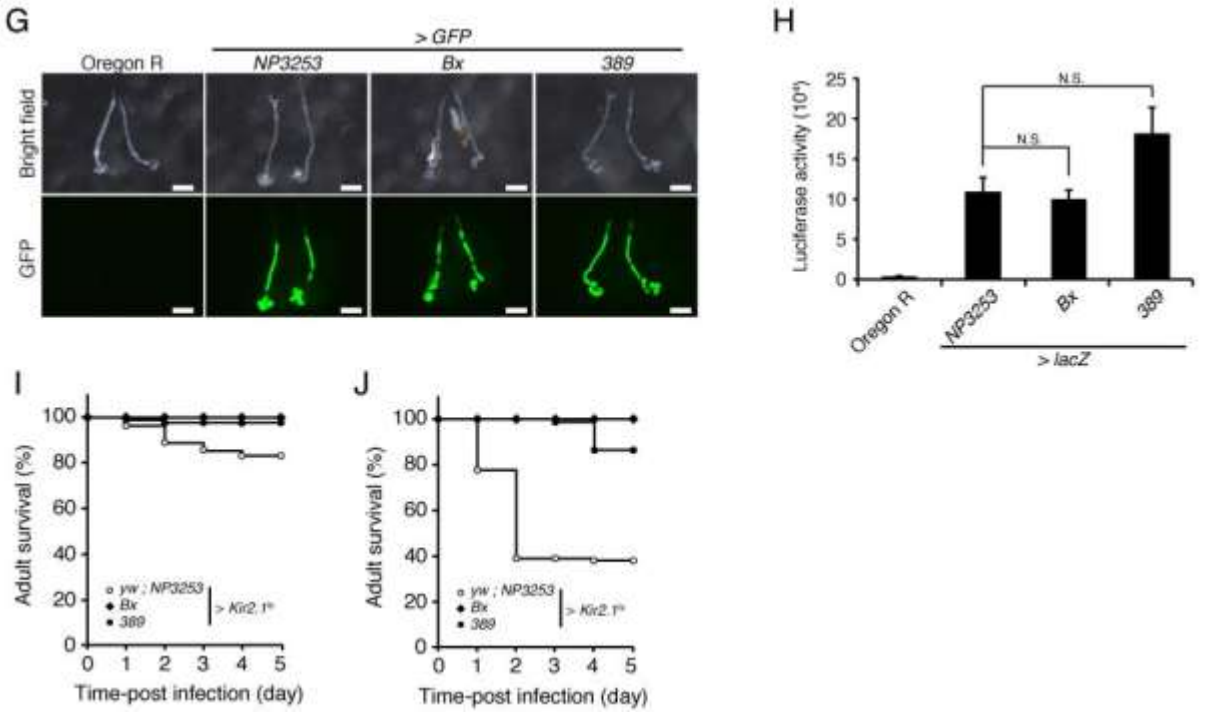

Figure. 2.

Some NP3253-positive cells are neurons responsible for the survival phenotype. **(A)** A schematic representation of the adult midgut. Red, green, blue, and yellow squares indicate the brain, proventriculus, anterior midgut, and posterior midgut, respectively. **(B)** Fluorescent confocal imaging of *NP3253>mCD8::GFP* flies. Green indicates NP3253-positive cells (anti-GFP). Blue indicates nuclei (DAPI). Red indicates visceral muscles (phalloidin). Arrowheads indicate NP3253-positive cells that appear to innervate epithelial cells. Bars, 20 μm. **(C)** Fluorescent confocal imaging of the proventriculus or posterior midgut of *NP3253>mCD8::GFP* flies. Green indicates NP3253-positive cells (anti-GFP). Blue indicates visceral muscles (phalloidin). Red indicates neuronal marker (anti-HRP). Bar, 50 μm. **(D**) Characterization of NP3253-positive cells by neuronal markers. Fluorescent confocal imaging of *NP3253>DenMark, syt.eGFP* flies. Green indicates synaptic vesicles (anti-GFP). Blue indicates neurons (anti-HRP). Red indicates DenMark (anti-RFP). Bars, 20 μm except for the lowest panels (10 μm). (**E**) Fluorescent confocal imaging of *NP3253>DenMark, syt.eGFP* flies. Green indicates synaptic vesicle (anti-GFP). Blue indicates nuclei (DAPI). Red indicates DenMark (anti-RFP). Bars, 20 μm. **(F)** Survival analysis of flies orally infected with *Ecc15-GFP*. lacZ or Kir2.1 is driven by NP3253-GAL4,

together with (filled symbols) or without (open symbols) elav-GAL80. *NP3253* is w^{1118} background (left) or *y w* background (right). $P<0.0001$ (left and right, comparing *NP3253>Kir2.1* with *elav-GAL80; NP3253>Kir2.1*). Each survival curve corresponds to at least 2 independent experiments of 3 tubes of 30 flies each. *P* values were calculated with the log-rank test. **(G)** Survival analysis with salivary gland GAL4 drivers. Whole-salivary gland imaging of GFP-expressed flies by several GAL4 drivers. Salivary glands were observed under a light microscope (upper) or fluorescence microscope (lower). Green indicates GFP signal. Bars, 200 µm. **(H)** Measurement of lacZ activity by β-glo assay. Five flies were examined and the graph shows a representative result of two independent experiments (N.S., not significant: $p>0.05$). **(I)** Survival analysis of Kir2.1-expressing flies by Bx-GAL4 or 389-GAL4 lines without infection. **(J)** Survival analysis of Kir2.1-expressing flies by Bx-GAL4 and 389-GAL4 lines upon oral infection with *Ecc15-GFP*. No infection indicates sucrose feeding after starvation. Each survival curve corresponds to at least 2 independent experiments of 3 tubes of 30 flies each. *P* values were calculated with the log-rank test ($p<0.01$).

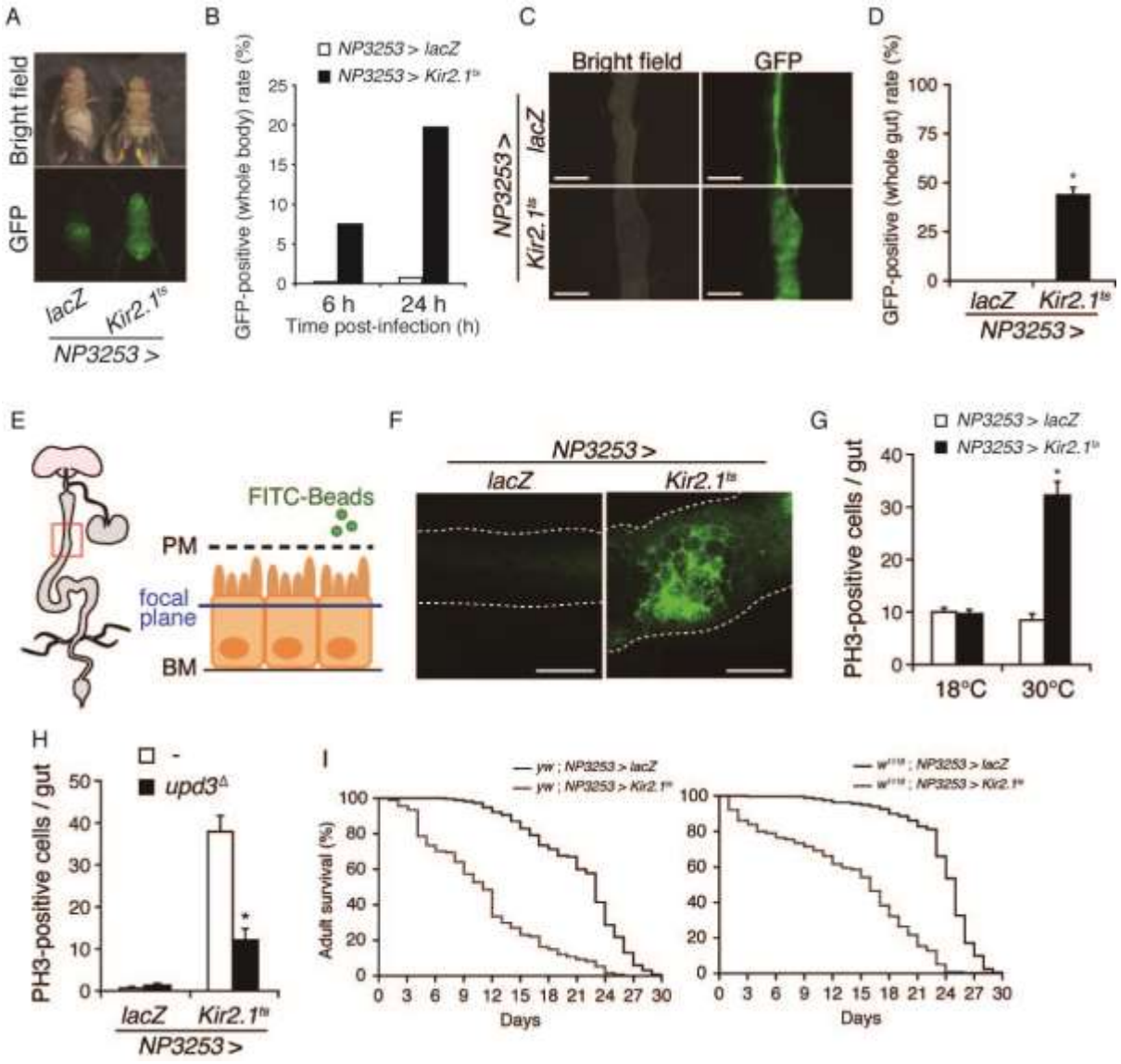

Figure. 3.

Increased permeability of gut barriers in *NP3253>Kir2.1* flies. **(A)** Whole-body imaging of *NP3253>Kir2.1* flies that ingested *Ecc15-GFP*. Flies were observed under a light microscope (upper) or fluorescence microscope (lower). Green indicates GFP signal. **(B)** Statistical analysis of (A). The number of flies that show GFP signals in the whole body 6 h or 24 h after ingestion was counted and is shown as a percentage. Approximately 100 flies were examined and the graph shows representative results of two independent experiments. **(C)** Bead-feeding assay of *NP3253>Kir2.1* flies. Adult flies were fed FITC-labeled latex

beads with a 50-nm diameter. Guts were dissected and examined under a conventional fluorescence microscope. The picture shows the anterior part of the midgut. FITC signals are retained in the lumen if the dextran beads cannot pass through the peritrophic matrix. Note that FITC signals were diffuse in *NP3253>Kir2.1* flies. Bars, 200 µm. **(D)** Statistical analysis of (C). The number of flies with FITC signal in the whole anterior midgut 10 min after feeding was counted and is shown as a percentage. 20-30 flies were examined and the graph shows a representative result of three independent experiments (*: $p<0.05$). **(E)** A schematic representation of the dextran-feeding assay with a confocal microscope. The left panel shows the adult midgut and the red square indicates the examined part in (F). The right panel presents the cross section of the adult midgut and the focal plane that was scanned by a confocal microscope in (F). PM, peritrophic matrix. BM, basement membrane. **(F)** Fluorescent confocal imaging of *NP3253>mCD8::GFP* flies and *NP3253>Kir2.1* flies fed FITC-labeled latex beads. Green indicates FITC signals. Broken line shows the gut outline. Bars, 50 µm. **(G)** The number of PH3-positive cells per one adult midgut in *NP3253>Kir2.1* flies. The flies were kept at 30℃ for 2 days, and their guts were dissected and stained with anti-PH3 antibody. PH3 signals were counted under a confocal microscope. 10-12 flies were examined and the graph shows the average of three independent experiments (*: $p<0.05$). **(H)** PH3-positive cells in *upd3* mutant background flies. 10 to 12 flies were examined and the graph shows representative results of two independent experiments (*: $p<0.05$). **(I)** Lifespan analysis. Survival analysis of *yw ; NP3253>lacZ* or *NP3253>Kir2.1* flies at 30℃ (left), or w^{1118} *; NP3253>lacZ* or *NP3253>Kir2.1* flies at 30℃ (right). Each survival curve corresponds to at least 3 independent experiments of 3 tubes of 30 flies each. *P* values were calculated with the log-rank test ($p<0.0001$).

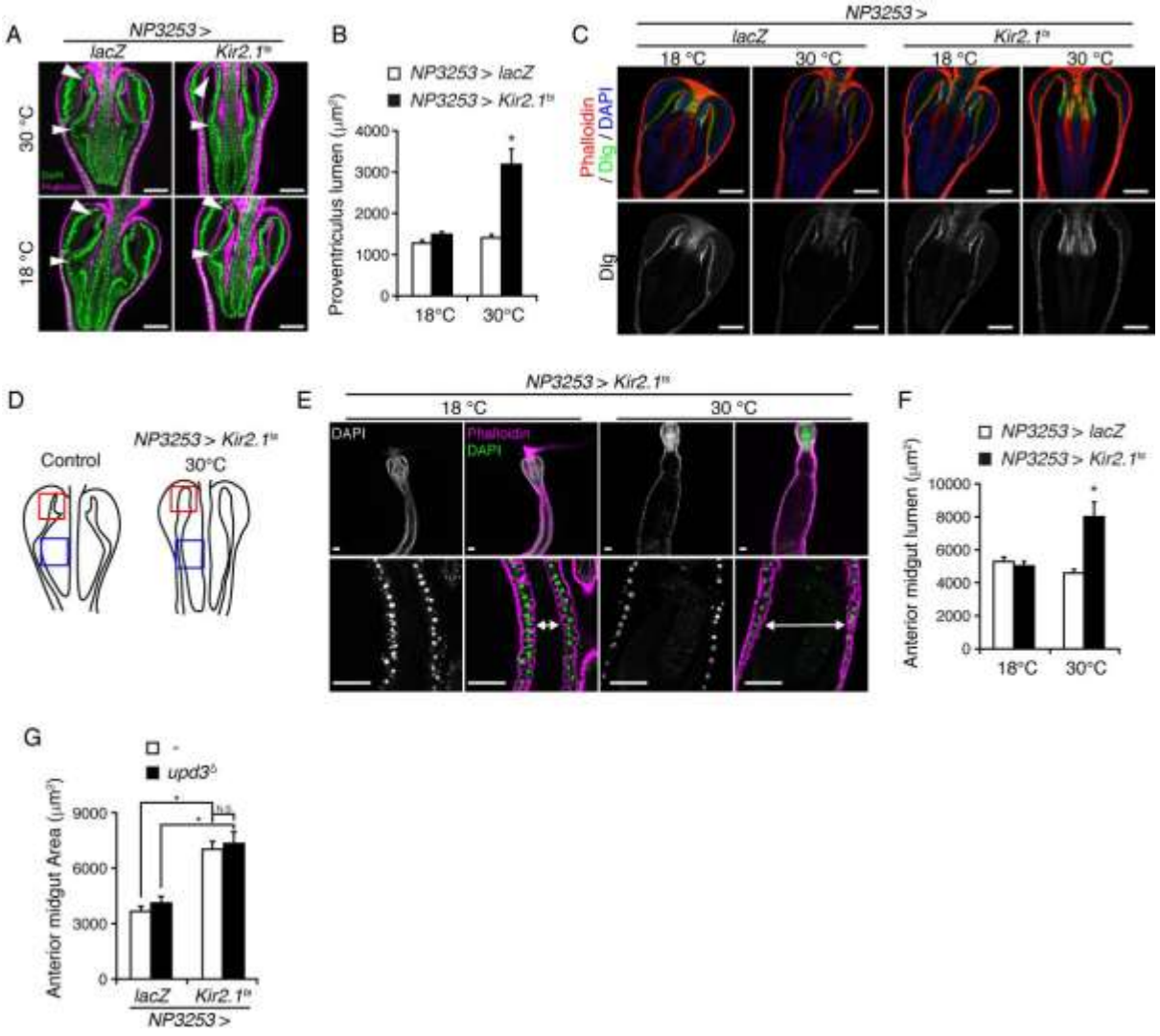

Figure. 4.

Aberrant gut structure of *NP3253>Kir2.1* flies. **(A)** Fluorescent confocal imaging of the proventriculus of *NP3253>Kir2.1* flies. Green indicates nuclei (DAPI). Magenta indicates visceral muscles (phalloidin). Arrowheads and arrows indicate areas of the proventriculus of *NP3253>Kir2.1* flies with an abnormal structure. Bars, 50 μm. **(B)** Statistical analysis of (A). An area of the luminal region of the proventriculus was measured by ImageJ. 16-25 flies were examined and graph shows representative results of two independent experiments (*: $p<0.05$). **(C)** Fluorescent confocal imaging of the proventriculus of *NP3253>Kir2.1* flies. Green indicates a marker of septate junctions (anti-discs-large). Blue indicates nuclei (DAPI).

Red illustrates visceral muscles (phalloidin). Lower panels show anti-discs-large signals in the upper panels. Bars, 50 μm. **(D)** Schematic representation of the interpretation of (A) and (C). Red squares indicate the location of arrows in (A). Blue squares show the location of arrowheads in (A). **(E)** Fluorescent confocal imaging of the anterior midgut of *NP3253>Kir2.1* flies. Magenta indicates visceral muscles (phalloidin). Green or white indicate nuclei (DAPI). Arrows indicate the luminal width of the anterior midgut. Lower panels show the magnified view of the upper panels. Bars, 50 μm. **(F)** Statistical analysis of (E). An area of anterior midgut (from the top of the proventriculus to the 200-μm point) was measured by Image J. 16-25 flies were examined and the graph shows representative results of two independent experiments (*: $p<0.05$). **(G)** Fluorescent confocal imaging of the anterior midgut was obtained in the same way as in Fig 4E, and an area of anterior midgut (from the top of the proventriculus to the 200 μm point) of *NP3253>Kir2.1* flies was measured by Image J. 16-25 flies were examined and the graph shows representative results of two independent experiments (*: $p<0.05$).

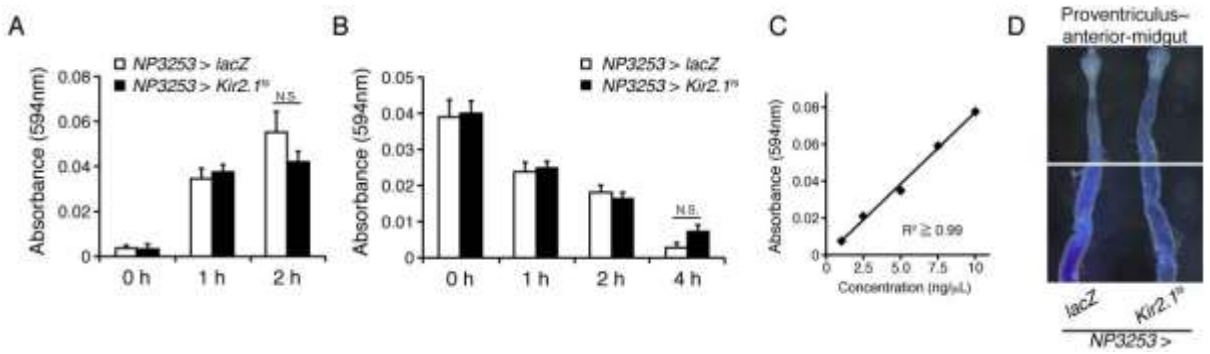

Figure. 5.

Feeding assay with BPB-containing food. **(A)** Measurement of the feeding amount. Starved *NP3253>Kir2.1* flies were fed food containing 0.5% BPB for the indicated period, and whole flies were homogenized and absorption at 594 nm was measured. Three tubes of three flies each were examined and the graph shows a representative result of three independent experiments. (N.S. : $p>0.05$). **(B)** Measurement of the excretion rate. Starved *NP3253>Kir2.1* flies were fed with food containing 0.5% BPB for 1 h, changed to normal food for the indicated period, and whole flies were homogenized and absorption at 594 nm was measured. Three tubes of five flies each were examined and the graph shows representative results of three independent experiments (N.S. : $p>0.05$). **(C)** Calibration curve for BPB measurement. The standard curve for 594 nm absorption between 0.01 to 0.08 was $R^2 \geqq 0.99$. **(D)** Microscopic observation of the midgut of BPB-fed flies. Proventriculus-anterior midguts and middle-posterior midguts were observed under a light microscope. Blue indicates BPB signal.

Table 1

The list of enhancer trap lines screened in this study. The enhancer trap lines in this list were crossed with *tubP-GAL80^{ts}* ; *UAS-Kir2.1-EGFP* flies, and survival after oral infection with *Ecc15-GFP* was examined. These lines induce expression in the brain. The stock number and stock centers are shown.

#	Flytrap #	#	Bloomington #	#	DGRC #	#	Others
1	c219	111	8848	212	112-107	344	NP21
2	129y	112	9150	213	112-468	345	NP3020
3	c240	113	7469	214	112-898	346	NP873
4	66y	114	33825	215	112-800	347	fru-GAL4
5	c164	115	32555	216	113-025		
6	71y	116	30819	217	103-871		
7	c536b	117	8767	218	112-171		
8	c367	118	35543	219	104-210		
9	c61	119	7026	220	112-424		
10	7y	120	25410	221	112-636		
11	c123a	121	8746	222	112-788		
12	c44a	122	30833	223	104-313		
13	c365a	123	30828	224	112-027		
14	c857	124	7148	225	112-338		
15	c232	125	3740	226	103-954		
16	c217	126	30846	227	112-162		
17	c210	127	32550	228	104-190		
18	c712	128	7365	229	104-309		
19	c187	129	9464	230	112-450		
20	10y	130	32545	231	104-266		
21	c259	131	8641	232	104-219		
22	c704	132	30822	233	112-043		
23	c288	133	30831	234	103-640		
24	c284b	134	3741	235	103-985		
25	c67	135	6480	236	104-355		
26	9y	136	30845	237	112-021		
27	171y	137	6982	238	112-095		
28	c283	138	31425	239	103-744		
29	c105	139	3797	240	112-292		
30	c508	140	6798	241	112-912		
31	c753	141	8849	242	103-518		
32	c300	142	30814	243	112-926		
33	c309a	143	33807	244	112-198		
34	c187	144	30832	245	103-867		
35	106y	145	7023	246	112-886		
36	36y	146	24147	247	112-282		
37	201y	147	24903	248	112-286		
38	156y	148	6902	249	112-170		
39	93y	149	30829	250	112-976		
40	116	150	7009	251	112-712		
41	c282	151	30818	252	112-445		
42	11y	152	30835	253	112-462		
43	c205	153	27636	254	103-887		
44	c755	154	30546	255	112-482		
45	c249	155	9462	256	113-070		
46	62y	156	33823	257	112-663		
47	21y	157	30830	258	104-173		
48	c228	158	7127	259	103-940		
49	c65	159	30839	260	112-511		
50	c632c	160	9465	261	104-218		
51	43y	161	30849	262	112-829		
52	c887	162	8764	263	112-537		
53	c119	163	6753	264	112-868		
54	c707	164	3733	265	103-583		
55	c282a	165	7415	266	113-044		
56	245y	166	7149	267	112-564		
57	242y	167	30836	268	112-470		
58	52y	168	30834	269	112-679		
59	c767	169	8768	270	113-037		
60	c505	170	8765	271	112-871		
61	c604a	171	30815	272	103-705		
62	c628	172	6906	273	112-875		
63	c837a	173	30840	274	112-303		
64	c229	174	6978	275	104-191		
65	c62	175	30813	276	103-923		
66	c874	176	6900	277	103-496		
67	c159b	177	33070	278	113-073		

Journal of Experimental Biology • Advance article

68	c172	**178**	25683	**279**	112–927		
69	c465	**179**	30823	**280**	105–377		
70	c118	**180**	8749	**281**	105–308		
71	c299	**181**	8474	**282**	114–174		
72	22y	**182**	30488	**283**	105–231		
73	c82	**183**	30838	**284**	114–253		
74	16y	**184**	32040	**285**	113–981		
75	c391	**185**	30816	**286**	105–257		
76	239y	**186**	30821	**287**	105–125		
77	c289	**187**	30812	**288**	105–171		
78	c609rc	**188**	25686	**289**	114–284		
79	64y	**189**	28801	**290**	105–481		
80	c41	**190**	30820	**291**	114–140		
81	213y	**191**	30554	**292**	104–818		
82	c593	**192**	6980	**293**	114–239		
83	c502	**193**	6871	**294**	114–145		
84	c182	**194**	30824	**295**	114–178		
85	c577a	**195**	30848	**296**	104–460		
86	17y	**196**	25685	**297**	114–084		
87	c855a	**197**	4669	**298**	113–133		
88	c983	**198**	26160	**299**	114–250		
89	c199a	**199**	6488	**300**	113–902		
90	c81	**200**	6301	**301**	105–311		
91	152y	**201**	9313	**302**	113–663		
92	187y	**202**	7009	**303**	104–816		
93	c819	**203**	6797	**304**	113–553		
94	c871	**204**	9263	**305**	114–088		
95	c492	**205**	26818	**306**	105–362		
96	210y	**206**	9580	**307**	113–956		
97	c189	**207**	7466	**308**	105–080		
98	c242	**208**	6980	**309**	105–258		
99	c747	**209**	6871	**310**	114–098		
100	c338	**210**	6488	**311**	105–355		
101	c758	**211**	6301	**312**	114–120		
102	c839			**313**	113–231		
103	c320a			**314**	113–327		
104	30y			**315**	114–164		
				316	**113–183**		
				317	104–844		
				318	113–812		
				319	114–200		
				320	113–659		
				321	104–931		
				322	105–073		
				323	105–486		
				324	114–131		
				325	113–657		
				326	114–060		
				327	113–185		
				328	113–545		
				329	113–961		
				330	104–414		
				331	113–160		
				332	104–937		
				333	113–140		
				334	105–423		
				335	104–360		
				336	113–683		
				337	114–282		
				338	104–906		
				339	113–359		
				340	114–143		
				341	105–401		
				342	113–629		
				343	105–426		

Journal of Experimental Biology • Advance article